Low-dosage Ozonation in Gas-phase Biofilter Promotes Community Diversity and Robustness.

Marvin Yeung
Tsinghua University School of Environment
Prakit Saingam
University of Hawai'i at Manoa Department of Civil and Environmental Engineering
Yang Xu
Tsinghua University School of Environment
Jinying Xi (xijinying@tsinghua.edu.cn)
Tsinghua University School of Environment https://orcid.org/0000-0002-1734-8973

Research

Keywords: Microbial community diversity, metabolic rates of different carbon sources

Posted Date: November 11th, 2020

DOI: https://doi.org/10.21203/rs.3.rs-58642/v3

Version of Record: A version of this preprint was published on January 12th, 2021. See the published version at https://doi.org/10.1186/s40168-020-00944-4.

Abstract

Background

The ozonation of biofilters is known to alleviate clogging and pressure drop issues while maintaining removal performances in biofiltration systems treating gaseous volatile organic compounds (VOCs). The effects of ozone on the biofilter microbiome in terms of biodiversity, community structure, metabolic abilities, and dominant taxa correlated with performance remain largely unknown.

Methods

This study investigated two biofilters treating high-concentration toluene operating in parallel, with one acting as control and the other exposed to low-dosage (200 mg/m^3) ozonation. The microbial community diversity, metabolic rates of different carbon sources, functional predictions, and microbial co-occurrence networks of both communities were examined.

Results

Consistently higher biodiversity of over 30% was observed in the microbiome after ozonation, with increased overall metabolic abilities for amino acids and carboxylic acids. The relative abundance of species with reported stress-tolerant and biofilm-forming abilities significantly increased, with a consortium of changes in predicted biological pathways, including shifts in degradation pathways of intermediate compounds, while the correlation of top ASVs and genus with performance indicators showed diversifications in microbiota responsible for toluene degradation. A co-occurrence network of the community showed a decrease in average path distance and average betweenness with ozonation.

Conclusion

Major degrading species highly correlated with performance shifted after ozonation. Increases in microbial biodiversity, coupled with improvements in metabolizing performances of multiple carbon sources including organic acids could explain the consistent performance commonly seen in the ozonation of biofilters despite the decrease in biomass, while avoiding acid buildup in long term operation. The increased presence of stress-tolerant microbes in the microbiome coupled with the decentralization of the co-occurrence network suggested that ozonation could not only ameliorate clogging issues but also provide a microbiome more robust to loading shock seen in full-scale biofilters.

Introduction

Biofiltration is a technology widely applied in the abatement of volatile organic compounds (VOCs) emissions. Biofilters are known for their low cost (Jorio et al., 1998; Metris et al., 2001; Strauss et al., 2004) and minimal secondary pollution (Iranpour et al., 2005; Deng et al., 2012). A persistent issue present in the application of biofilters is the excessive growth of biomass, resulting in clogging, increased pressure drop, and decreased removal performance (Alonso et al., 1997; Okkerse et al., 1999). Various biomass control methods have been developed to solve clogging issues (Yang et al., 2010). One technique of ozone injection was previously reported (Xi et al., 2014), complemented by another study examining the metabolic activities of the microbiome in biofilters under O_3 exposure, which concluded that O_3 exposure led to an increase in the metabolism of numerous carbon sources of lower biodegradability, such as γ-hydroxybutyric acid, d-galactonic acid γ -lactone, d-mannitol, d-cellobiose, and γ -methyl-d-glucoside. (Saingam et al., 2016). Traditionally O_3 is regarded as a strong oxidant that purges microorganisms and lowers overall biological activity (Fontes et al., 2012, Franzini et al., 2018). However, the opposite response was found in low-dosage O_3 exposure. For example, low concentrations of O_3 (e.g. 120 mg/m^3) were found to improve metabolic activity (Wang et al., 2009). It was shown that despite the decrease in biomass, microbial activity for the metabolism of multiple carbon sources increased in the biofilter, implying an inherent change at the microbial level. It is well known that the microbiome of a biofilter is crucial for effective pollutant abatement (Ralebitso-Senior et al., 2012), yet the exact microbiome and functional changes that occur allowing for increased microbial activity while maintaining system performance with a decrease in biomass remain intriguing and unknown. In this study, 16S rRNA sequences of the v4 region in a controlled biofilter and ozonated biofilter operated in parallel were sequenced in order to investigate the microbial changes leading to the adaptation and performance changes of the microbiome. Using statistical analysis techniques, we attempted to explain the relevance of dominant taxa treating toluene after addition of O_3. Using the latest databases, we predicted changes in functional and phenotypic characteristics under ozonation and quantified the relationship between microbiome change and removal performance.

Methodology

2.1 Experimental setup

Two lab-scale biofilters, BF1 and BF2, were constructed as acrylic cylinders with a 12 cm inner diameter and 25 cm height. Each biofilter was packed with porous perlite (0.54 void fraction) to form a 1.6-L filter bed with a height of 15.0 cm. An air compressor (Hailea ACO-318, Fuzhou, China) was used to feed air into the system. The gas flow rate was controlled by a flow meter (Zenxing LZD-4WB, Xianghu, China), leading into a sealed glass bottle containing liquid toluene to form mixed gas. A stainless-steel reactor equipped with a UV lamp (Cnlight ZW23D15W-Z436, Shenyang, China) was installed between the flow meter and the bottle containing liquid toluene, operating at 185 nm to produce gaseous ozone for BF1. For each biofilter, the packing media was initially mixed with 1.0 L of activated sludge collected from a municipal wastewater treatment plant (Xiaojiahe WWTP, Beijing, China). A nutrient solution containing $NaNO_3$ (20 g/L), Na_2HPO (1.6 g/L), and KH_2PO_4 (1.04 g/L) was sprayed directly on the filter beds of the two biofilters for sufficient humidity and nutrients. The leachate was discharged every day. The two biofilters were operated in parallel for 160 days in total. Both were operated in identical conditions without ozone for the first 44 days, and BF1 was fed with 200 mg/m^3 gaseous ozone after day 45.

2.2 Performance analytical methods

Gaseous toluene concentrations were measured using a gas chromatograph (SHIMADZU, GC-14C, Kyoto, Japan) with a flame ionization detector (GC/FID). The temperatures of the column, injector, and detector were set at 100, 150, and 150°C, respectively. The CO_2 level in the mixed gas sample was measured with an infrared detector (Testo, Testo 535 CO_2, Lenzkirch, Germany), and ozone concentration was monitored by a UV absorbance detector (2B Technologies Inc, 106-M, Boulder, USA).

All concentrations were measured daily at 9:00, 13:30, and 18:00 (GMT +8) with six replicates at each point. The highest and lowest replicate points were discarded, and the remaining four data replicates were averaged to yield three resulting data points for each day. Removal efficiency and mineralization rate data used in correlation analysis with the microbiome at a particular time point were obtained by averaging the performance data of three days surrounding the date of microbial sampling, including the day of sampling and one day before and after.

2.3 Microbial sampling

Microbial samples were taken from both biofilters at days 38, 52, 66, 80, 94, and 160. Packing media were taken from depths of 1, 7, and 15 cm of the filter bed and the biofilms were detached and suspended in phosphate buffer saline (PBS) by sonication at 425 W, 21–25 kHz for 10 min (Ningbo Science Biotechnology SCIENTZ-IID, Ningbo, China). The sonicated suspension was centrifuged at 10000 ×g for 1 min and resuspended in 5 ml PBS. To exclude dead cells within the community, a fluorescent dye (propidium monoazide, PMA) was used to treat the microbial suspension by inactivating the DNA of cells with damaged cell membranes as well as exposed DNA (Guo and Zhang, 2014). PMA (Biotum, PMA™ dye, Fremont, USA) stock was prepared by dissolving 1 mg PMA in 100 µL of 20% dimethyl sulfoxide (DMSO) and stored at −20°C; 2.5 µL of 20 mmol/L PMA solution was added into a 500 µL microbial suspension. The mixture was incubated at room temperature for 5 min and occasionally mixed. The tubes were placed horizontally on ice and exposed to a 650 W halogen light at a 20 cm distance for 4 min. Then, DNA from PMA-treated aliquots were isolated with the FastDNA® SPIN Kit for Soil (MP Biomedicals, Solon, USA) following the manufacturer's instructions.

Samples from days 66, 80, 94, and 160 were divided into three identical samples after PMA treatment and before DNA extraction, therefore each sample was represented in triplicate to counter systematic biases from DNA isolation, PCR and sequencing procedures. Samples from days 38 and 52 were not sequenced as triplicates and therefore were not included in all analyses of this study to ensure consistent biological and statistical validity. They were used only for verification of factual differences caused by ozone and not systematic errors, as seen in Supplementary Material 1.

2.4 High-throughput sequencing and data analysis

The primer 515F (5'-GTGCCAGCMGCCGCGGTAA-3') and reverse primer 806R (5'-GGACTACHVGGGTWTCTAAT-3') were used with 12 bp barcode (Invitrogen, Carlsbad, CA, USA) (Caporaso et al., 2011). PCR reactions, containing 25 µl 2x Premix Taq (Takara Biotechnology, Dalian, China), 1 µl of each primer (10 mM), and 3 µl DNA (20 ng/µl) template in a volume of 50 µl, were amplified by thermocycling: 95°C for 3 min, followed by 30 cycles of 98°C for 20 sec, 55°C for 15 sec, and 72°C for 15 sec, with a final extension at 72°C for 10 min. The PCR instrument used was a BioRad S1000 (Bio-Rad Laboratory, Irvine, USA). The length and concentration of the PCR product were detected by 1% agarose gel electrophoresis. Samples with bright main strips between 288–310 bp were used for further experiments. PCR products were mixed in equidensity ratios according to the GeneTools analysis software (Version4.03.05.0, SynGene). Then, the mixture of PCR products was purified with an EZNA gel extraction kit (Omega, Norcross, USA). Sequencing of the 16S rDNA V4 region was carried out on an Illumina Miseq platform. Barcodes and adapter sequences were trimmed with Cutadapt (Martin, 2011), then truncated at 210 bp and denoised with DADA2 to formulate the ASV (amplicon sequence variants) table (Callahan et al., 2016). Taxonomy of 16S rRNA sequences were classified with the Silva 16s rRNA database (release 138) at 99% similarity with the Naïve-Bayes algorithm for all analyses requiring taxonomy (Quast et al., 2013; ; Glick, et al., 2004). The software Bugbase was used for functional prediction, which required the Greengenes database, for which Greengenes (version 13_5) was used (Desantis et al., 2006). Function predictions were done using Bugbase and PICRUSt2 (version 2.1.2b) (Ward et al., 2017; Douglas et al., 2020). Statistical analyses, including alpha and beta analysis, were conducted in the R package Phyloseq (version 1.3) (McMurdie et al., 2013). The R package ALDEx2 (version 1.2) was used to statistically identify pathways highly specific to ozone and control biofilters (Fernandes et al., 2014). Correlation analyses were performed and plotted using Pearson correlation incorporated in the R package ggcor (Huang et al., 2020). Co-occurrence network analyses were conducted with the molecular ecological network analyses with Spearman correlation, Bray-Curtis dissimilarity, and an RMT (Random matrix theory) threshold of 0.81 (Deng et al., 2012). Networks were plotted with Java software Gephi (Bestian et al., 2009). All R packages were conducted under R version 3.6. LEfSe analysis was performed on the only galaxy platform maintained by the author, with p-value threshold of the Wilcoxon test set to 0.05 and LDA log-score threshold set to 3.0 (Segata et al., 2011).

2.4 Metabolic activity analysis

The suspension from sonification containing microbiomes detached from the packing media as described in Section 2.3 was diluted in PBS to obtain the optical density at 600 nm wavelength ($O.D._{600}$) at 0.05. The ECO plate (Biolog, Inc, Hayward, USA), with 31 various sources of carbon substrates mixed with tetrazolium dye, was prepared for the determination. Then, 150 µL of the microbial dilutions was inoculated to each well of the ECO plate and incubated at 30°C. The plate was observed for the absorbance at 600 nm regularly over a period of 3 days by the microplate reader (Molecular devices, Spectramax M5, San Jose, USA). The absorbance over time from wells containing carbon sources from the same group (e.g. amino acids) was averaged and the absorbance from the control well was deducted to avoid systematic error and obtain the average metabolic rates of different groups of carbon sources.

Results

3.1 Sequencing results

A total of 9347–59720 sequences of 210 bp were obtained. Samples were rarefied at 13,000 sequences, resulting in 24 samples. A total of 3295 ASVs were identified after denoising.

3.2 System performance

The effects of O_3 on performance data during the period was reported in detail in a previous publication (Saingam et al., 2018), in which both biofilters had a removal rate of approximately 65%–70% when treating inlet toluene ranging from 500 to 1500 mg/m^3, with no significant difference under t-test (p=0.62).

3.3 Biodiversity

Biodiversity indices comparing the two biofilters are shown in Fig.1. The observed intra-group diversity spanned over 400 ASVs in both groups, but the median and average diversity of the ozone biofilter were consistently higher than those of the control samples, indicating an increase in phylogenetic diversity range and average evenness.

3.4 Community differences and propensity of variables

A clear separation of microbiome composition was seen between the two biofilters. As the intra-group differences also fluctuated considerably with time, the relative abundances of major phyla *Actinobacteria, Proteobacteria, Firmicutes, Bacteroidetes*, and *TM7* were added as constraining variables in Fig. 2a to show the overall compositional differences in ASV levels and the abundance differences of major phyla. Detailed bar plots showing the relative abundances at all time points at the Phylum and Genus levels are provided in Supplementary Material 2. In addition to the prediction of microbiome functions, microbiome phenotypic metabolizing activity from Biolog ECO plates was adopted as constraining variables to show the preference of communities for different carbon sources in Fig 2b. *Proteobacteria* remained dominant in relative abundance after ozonation; *Firmicutes* were increased after ozonation, consisting mostly of gram-positive species; and *Actinobacteria,* another Phylum with mostly gram-positive species, were suppressed after ozonation. The metabolization ability of groups of amino acids and carboxylic acids increased in the microbiome under ozonation, each containing a consortium of numerous compounds from the groups, while metabolization rates for complex carbohydrates decreased. The metabolization data of individual compounds are provided in Supplementary Material 3.

3.5 Functional characteristics and traits caused by ozonation

The phenotypic traits of the microbiome from both biofilters are shown in Fig. 3. Increases in aerobic, gram-negative, pathogenic, biofilm forming, and stress-tolerant species were seen after ozonation, while species with flagellum mobility decreased.

MetaCyc pathways predicted by PICRUSt2 that changed substantially with an ALDEx effect size of over 2.5 are shown in Fig. 4. Among 15 pathways highly specific to ozonation, mycolate biosynthesis, taxadiene biosynthesis (engineered), the superpathway of heme biosynthesis from glycine, and (5Z)-dodec-5-enoate biosynthesis are crucial pathways for the assembling of proteins for cell membrane synthesis. Although gram-negative bacteria increased with ozonation, the repair and synthesis of cell membranes to mitigate oxidative disruption due to ozone was seen in the microbiome, along with the production of antioxidants such as heme and UDP-glucose-derived O-antigen biosynthesis. Of all enriched pathways after ozonation, the phenylacetate degradation I (aerobic) pathway was the most significant with an effect size of over 2.5. Phenylacetate and the degradation of other compounds containing acetate groups are widely seen in the essential steps of toluene and xylene degradation, two recalcitrant compounds commonly seen as VOCs pollutants (Vardar et al. 2004, Leutwein et al. 2001).

A decrease in pathways from the TCA cycle was seen in ozonation filter, and pathways for the degradation of other metabolites in VOCs degradation such as 3-phenylpropanoate and inositol increased after ozonation, indicating a variety of nonuniform changes in pathways. No decisive changes affecting the overall functional degrading ability were seen between groups, but rather a mixture of pathway changes, most of which were specific to particular metabolites before complete mineralization.

3.6 Correlation of system performance and dominant taxa

Due to the high functional redundancy known in bacterial populations, the majority of functions are commonly assumed to be performed by the most abundant taxa in a certain microbiome (Escalas et al., 2019). The dominant taxa on both ASV and genus level with top 20 relative abundance were selected, and their abundance in different samples and operation time were plotted with the removal efficiency and mineralization rates of corresponding samples in order to investigate differences and similarities in the reactions of dominant taxa and their relationship with performance measures, as shown in Fig. 5. By comparing both removal efficiency and mineralization rate, insights can be drawn from the removal of toluene and the complete degradation to CO_2 and hence intermediate metabolites.

Both the correlation of ASV and genus level phenylacetate were chosen to investigate possible intra-genus differentiation and radicality of differences. Nine out of 20 genera were always correlated with removal efficiency in both ozone and control biofilter, whereas only 3 out of 20 ASVs were always correlated with removal efficiency, indicating a high specificity and different reaction of ASVs in the same genus toward ozonation. All four ASVs from the genus Rhodococcus present in this system were strongly proportional with removal efficiency in the control biofilter but negatively correlated with removal efficiency in the ozonated biofilter.

3.7 Topological analysis andco-occurrence network construction of microbiome

Two co-occurrence networks were constructed with 91 and 107 nodes, 146 and 256 links, and 5.1 and 3.6 average path distances for the control and ozone biofilters, respectively, with the increase of average degree from 3.2 to 4.7, respectively, under identical specifications for network construction, as seen in Fig.

6. A more connected and even network was seen in the ozone microbiome; a network with shorter path distances coupled with smaller centralization of betweenness is commonly seen as more stable, as the major hubs are more diverged and less nodes are likely to be affected by shocks. Major hubs in the control biofilter such as ASV68 and ASV309 were substantially irrelevant in the ozone biofilter, indicating a radical change in the microbial network and hub distribution, yet ASV26, corresponding to the genus *Pandoreae*, remained highly relevant in betweenness and degree count in both systems. Exact ASV taxonomic assignments can be seen in Supplementary Material 4.

Discussion

Pollutant removal performance is the main goal of improvement attempts with regards to alleviating clogging issues. Numerous studies have reported that ozonation improves or maintains VOCs removal performance while significantly reducing biomass growth rates (Xi et al., 2015, Maldonado-Diaz and Arriaga, 2015; Wang et al., 2009). The results from our study, conducted for a period of 160 days, were consistent with those of previous studies in that no statistically significant changes were seen in terms of removal efficiency when operating at a relatively higher loading rate (fluctuating between 20–70 mg/L/h) compared to usual full-scale applications, showing ozonation to be a suitable candidate for full-scale application with the ease of retrofitting and flexible manipulation, as ozone can be easily mixed with the inlet gas flow.

Oxidative stress such as ozonation is known to reduce diversity and induce strong bactericidal effects at higher dosages (e.g. 5000 – 20000 mg/m^3), but our results showed the opposite, possibly due to a low-enough dosage to allow the subsistence of strains more sensitive to oxidative stress while stimulating the more robust strains, resulting in a more diverse microbiome (Fontes et al., 2012, Franzini et al., 2018). Given the diverse nature of xenobiotic degradation pathways, and the complexity of pollutant composition frequently seen in full-scale applications, ozonation is a possible method for the steady stimulation of microbiome diversity. Microbiome diversity has been reported to correlate directly with community stability and resistance to shocks, which are most commonly seen as spikes in loading rates during periods spanning from hours to months in full-scale operations depending on the particular scenario ((Hillebrand et al., 2008; Yang et al., 2008). The microbial co-occurrence network is a common modelling approach for describing characteristics and patterns of microbial co-occurrences, and indicating ecological processes governing community structures (Lima-Mendez et al., 2015). The co-occurrence networks shown in Fig. 6 also support the hypothesis that the ozonated microbiome may be more resilient to shocks with a more decentralized microbiome network after ozone injection, resulting in a community structure less likely to experience changes as radical as there would be in the more centralized network of the control biofilter microbiome.

After ozonation, a series of microbes in the phylum *Proteobacteria* increased in relative abundance, most prominently including genera *Dokdonella* and *Mesorhizobium*. *Dokdonella* was identified as a major effective degrader of styrene in biofilters (Portune et al., 2020). *Mesorhizobium* is an genus containing species strongly correlated to nitrogen fixation and denitrification with aerobic respiration, yet the genus was uncommonly reported to be associated with gaseous biofilters, correlation analysis of *Mesorhizobium*'s relative abundance and performance as seen in Fig.5a shows that the genus strongly correlates with mineralization rate of the biofilter after ozonation, this could be explained by enhanced effective use of nitrogen sources through nutrient spraying (Delgado et al., 2007). *Proteobacteria* in general has been widely reported to contain the dominant degraders of xenobiotics in both biofilter and wastewater treatments (Allievi et al., 2018, Van der Heyden et al., 2019). *Proteobacteria* has also been reported to have a higher presence in the treatment of more complex pollutants and higher loading stress, inducing higher functional diversity (Friedrich and Lipski 2010). A full list of families and genera that changed significantly with ozonation identified by LEfSe analysis can be seen in Supplementary Material 5. The degradation of xenobiotics such as toluene had highly diverse prokaryotic pathways and different degrading communities have different abilities and propensity for metabolizing different parts of the pathway before final mineralization of VOCs (Vallero, 2008). A more even and less specialized phenotypic functional profile may be desirable in full-scale applications when the composition of pollutants fluctuates widely and contains a variety of VOCs groups, though this decreased metabolization rate of complex carbohydrate degradation and increases in other compounds caused by ozonation did not impinge the removal efficiency of the biofilter.

An increase in the stress tolerance of the microbiome is highly desirable in biofilters because common applications of biofilters include the emission of periodic fermentation, and highly diverse pollutants are produced by the chemical engineering and pharmaceutical industries depending on the production agenda. Such variations in the inlet introduce shocks and hinder the performance of biofilters by eliminating degrading strains unfit for the new environment (Cabrol and Malhautier 2011). The consistently increased stress-tolerant strains after ozonation will maintain performance and could mitigate such shocks in full-scale situations to an extent, a highly desirable outcome. An increase in the biofilm-forming population could be an issue in traditional biofilters with clogging issues, but the ozonation of biofilters was shown to greatly reduce the growth rate of overall biomass and alleviate pressure drop. The increase in the biofilm-forming population should therefore not be considered a hindrance to the steady operation of biofilters after the inoculation phase.

Functional predictions on the pathway level provided us with microscopic views of the microbiome function. Attesting to predicted phenotypic traits, increases in pathways responsible for cell membrane synthesis as a response to oxidative stress corresponded with shifts in different parts of toluene degradation pathways. Purine ribonucleoside degradation feeding the urea cycle along with aspartate degradation and pyrimidine deoxyribonucleosides degradation all contributed to the degradation of amino acids, indicating increased metabolic rates for carbon sources such as amino acids. Although not a targeted substrate for the microbiome in this study, organic acids are seen as toxic metabolites that build up in biofilters during long term operation and periodic neutralization is required to maintain the health of the degrading community (Vallero, 2008).. Increases in metabolic activity indicated by enrichment in acid degrading pathways is an advantage for biofilters with regards to lessening organic acid buildups.

Correlation analysis of performance and microbes showed that the commonly seen genus *Rhodococcus* negatively correlated with performance after ozonation. As numerous studies have reported that this genus is dominant in the degradation of xenobiotics in biofilter systems (Portune et al., 2015, Allievi et al., 2018), this indicated a shift in degrading contribution away from *Rhodococcus* and more toward ASVs from the genera *Devosia, Aquamicrobium*, and *Rhizobiales*, which had high positive correlation with performance. The genus *Pandoreae* was reported to be highly enriched in species capable of effective

degradation of xenobiotics (Peeters et al., 2019), and was positively correlated with r>0.7 in both biofilters as shown in Fig. 6. Similar trends in these three genera were seen at the combined genus level.

The ozonation of biofilters has been shown to alleviate clogging issues while maintaining performance. This study revealed other potential improvements to the microbiome due to ozonation such as higher biodiversity and functional stability, attested by a more connected and robust topological network with less centralized distribution and lower average path, and a higher percentage of the microbiome being stress tolerant while phenotypically achieving higher metabolization rates for a variety of carbon sources. These factors all contribute to shaping a more robust and shock-resistant microbiome. Improving the microbiome is another positive aspect of ozone application along with the ease of retrofitting and solving clogging issues in full-scale applications.

Conclusion

Shifts in major degrading species corresponding to performance, as well as increases in community biodiversity could explain the consistent performances commonly seen in ozonation of biofilters despite the decrease in biomass. Increased metabolic activities of the ozonated microbiome for organic acids could ameliorate toxic accumulation issues present in long-term biofilter operation. The increased presence of stress-tolerant microbes as well as results from co-occurrence networks suggest that ozonation could not only mitigate clogging issues but also provide a microbiome more robust to loading shocks, which is desirable in full-scale biofilters. Additionally, functional predictions showed shifted pathway inclinations towards different parts of the toluene degradation pathway, and increased cell-membrane synthesis after ozonation. This study revealed numerous characteristics induced by ozone on the biofilter microbiome that explain the overall improvements in performances.

Declarations

Availability of data and materials: Sequence data of all samples are available at: GenBank BioProject accession number PRJNA656689. Codes used for statistical analysis and plotting can be accessed at*: https://github.com/myhyeung/Low-Dose-Ozonation-in-Gaseous-VOCs-Biofilter-Promotes-Community-Diversity-and-Robustness.*

Funding: This study was supported by the National Natural Science Foundation of China (No. 52070113), and the Major Science and Technology Program for Water Pollution Control and Treatment of China (No. 2011ZX07301-003).

Conflicts of Interest: The authors declare no conflict of interest.

Ethics approval and consent to participate: Not applicable

Consent for publication: Not applicable

Competing interests: The authors declare that they have no competing interests

Authors' contributions: MY performed analysis of the data and was the sole contributor in writing the manuscript. PS performed the operation and experiments of the biofilters and sampling. XY provided guidance and help during operation and sampling. JX is the corresponding author and provided funding, guidance, facilities for this study.

Acknowledgements: We thank Dr. Dao Guohua for his help on this project.

References

1. Auffret, M., Labbé, D., Thouand, G., Greer, C.W., Fayolle-Guichard, F., 2009. Degradation of a mixture of hydrocarbons, gasoline, and diesel oil additives by Rhodococcus aetherivorans and Rhodococcus wratislaviensis. Appl. Environ. Microbiol. 75 (24), 7774–7782.
2. Yang, Chunping & Chen, Hong & Zeng, Guangming & Yu, Guanlong & Luo, Shenglian. (2010). Biomass accumulation and control strategies in gas biofiltration. Biotechnology advances. 28. 531-40. 10.1016/j.biotechadv.2010.04.002.
3. Berenjian, A., Chan, N., Malmiri, H.J., 2012. Volatile organic compounds removal methods: a review. Am. J. Biochem. Biotechnol. 8 (4), 220–229.
4. Cape, J.N., 2003. Effects of airborne volatile organic compounds on plants. Environ. Pollut. 122 (1), 145–157.
5. Cox, H.H., Deshusses, M.A., 1999. Biomass control in waste air biotrickling filters by protozoan predation. Biotechnol. Bioeng. 62 (2), 216–224.
6. Delhoménie, M.C., Bibeau, L., Gendron, J., Brzezinski, R., Heitz, M., 2003. A study of clogging in a biofilter treating toluene vapors. Chem. Eng. J. 94 (3), 211–222.
7. Dorado, A.D., Baeza, J.A., Lafuente, J., Gabriel, D., Gamisans, X., 2012. Biomass accumulation in a biofilter treating toluene at high loads–Part 1: Experimental performance from inoculation to clogging. Chem. Eng. J. 209, 661–669.
8. Dosti, B., Guzel-Seydim, Z.E.Y.N.E.P., Greene, A.K., 2005. Effectiveness of ozone, heat and chlorine for destroying common food spoilage bacteria in synthetic media and biofilms. Int. J. Dairy Technol. 58 (1), 19–24.
9. Caspi et al 2018, "The MetaCyc database of metabolic pathways and enzymes", Nucleic Acids Research 46(D1):D633-D639
10. Allievi, M. J., et al. (2018). "Bacterial community diversity in a full scale biofilter treating wastewater odor." Water Sci Technol 77(7-8): 2014-2022.
11. Cabrol, L. and L. Malhautier (2011). "Integrating microbial ecology in bioprocess understanding: the case of gas biofiltration." Appl Microbiol Biotechnol 90(3): 837-849.

12. Caporaso, J. G., et al. (2011). "Global patterns of 16S rRNA diversity at a depth of millions of sequences per sample." Proc Natl Acad Sci U S A 108 Suppl 1: 4516-4522.
13. Escalas, A., et al. (2019). "Microbial functional diversity: From concepts to applications." Ecol Evol 9(20): 12000-12016.
14. Fernandes, A. D., et al. (2014). "Unifying the analysis of high-throughput sequencing datasets: characterizing RNA-seq, 16S rRNA gene sequencing and selective growth experiments by compositional data analysis." Microbiome 2: 15.
15. Fontes, B., et al. (2012). "Effect of low-dose gaseous ozone on pathogenic bacteria." BMC Infect Dis 12: 358.
16. Franzini, M., et al. (2018). "Microbiological aspects of ozone: bactericidal activity and antibiotic/antimicrobial resistance in bacterial strains treated with ozone." Ozone Therapy 3(3).
17. Friedrich, M. M. and A. Lipski (2010). "Characterisation of hexane-degrading microorganisms in a biofilter by stable isotope-based fatty acid analysis, FISH and cultivation." Appl Microbiol Biotechnol 85(4): 1189-1199.
18. Peeters, C., et al. (2019). "Comparative Genomics of Pandoraea, a Genus Enriched in Xenobiotic Biodegradation and Metabolism." Front Microbiol 10: 2556.
19. Portune, K. J., et al. (2015). "Investigating bacterial populations in styrene-degrading biofilters by 16S rDNA tag pyrosequencing." Appl Microbiol Biotechnol 99(1): 3-18.
20. Portune, K. J., et al. (2020). "Contribution of bacterial biodiversity on the operational performance of a styrene biotrickling filter." Chemosphere 247: 125800.
21. Segata, N., et al. (2011). "Metagenomic biomarker discovery and explanation." Genome Biol 12(6): R60.
22. Van der Heyden, C., et al. (2019). "Long-term microbial community dynamics at two full-scale biotrickling filters treating pig house exhaust air." Microb Biotechnol 12(4): 775-786.
23. Yoshikawa, M., et al. (2016). "Enhancement and Biological Characteristics Related to Aerobic Biodegradation of Toluene with Co-Existence of Benzene." Water, Air, & Soil Pollution 227(9).
24. Bolyen, E., Rideout, J. R., Dillon, M. R., Bokulich, N. A., Abnet, C. C., Al-Ghalith, G. A., ... & Bai, Y., 2019. Reproducible, interactive, scalable and extensible microbiome data science using QIIME 2. Nature biotechnology 37, 852-857.
25. Callahan, B.J., Mcmurdie, P.J., Rosen, M.J., Han, A.W., Johnson, A.J.A., Holmes, S.P., 2016. Dada2: high-resolution sample inference from illumina amplicon data. Nature Methods 13, 581-583.
26. Louca, S., Parfrey, L.W., Doebeli, M., 2016. Decoupling function and taxonomy in the global ocean microbiome. Science 353, 1272-1277.
27. Martin, M., 2011. Cutadapt removes adapter sequences from high-throughput sequencing reads. EMBnet. journal 17, 10-12.
28. Rognes, T., Flouri, T., Nichols, B., Quince, C., & Mahé, F., 2016. VSEARCH: a versatile open source tool for metagenomics. Peer J 4, e2584.
29. Glick, M., Klon, A. E., Acklin, P., & Davies, J. W., 2004. Enrichment of extremely noisy high-throughput screening data using a naive Bayes classifier. Journal of biomolecular screening 9, 32-36.
30. T.Z. DeSantis, P. Hugenholtz, N. Larsen, M. Rojas, E.L. Brodie, K. Keller, T. Huber, D. Dalevi, P. Hu, G. L. Andersen. 2006. Greengenes, a Chimera-Checked 16S rRNA Gene Database and Workbench Compatible with ARB. Applied and Environmental Microbiology 72 (7) 5069-5072; DOI: 10.1128/AEM.03006-05
31. Quast C, Pruesse E, Yilmaz P, et al. The SILVA ribosomal RNA gene database project: improved data processing and web-based tools. Nucleic Acids Res. 2013;41(Database issue):D590-D596. doi:10.1093/nar/gks1219
32. Ralebitso-Senior, T. Komang & Senior, Eric & Di Felice, Renzo & Jarvis, Kirsty. (2012). Waste Gas Biofiltration: Advances and Limitations of Current Approaches in Microbiology. Environmental science & technology. 46. 8542-73. 10.1021/es203906c.
33. McMurdie PJ, Holmes. 2013. phyloseq: An R Package for Reproducible Interactive Analysis and Graphics of Microbiome Census Data. phyloseq: An R Package for Reproducible Interactive Analysis and Graphics of Microbiome Census Data
PLOS ONE 8(4): e61217. https://doi.org/10.1371/journal.pone.0061217
34. Tonya Ward, Jake Larson, Jeremy Meulemans, Ben Hillmann, Joshua Lynch, Dimitri Sidiropoulos, John.R. Spear, Greg Caporaso, Ran Blekhman, Rob Knigł BugBase predicts organism-level microbiome phenotypes. doi: https://doi.org/10.1101/133462
35. Nhu H. Nguyen, Zewei Song, Scott T. Bates, Sara Branco, Leho Tedersoo, Jon Menke, Jonathan S. Schilling, Peter G. Kennedy, FUNGuild: An open annotation tool for parsing fungal community datasets by ecological guild, Fungal Ecology, Volume 20, 2016, Pages 241-248, ISSN 1754-5048, https://doi.org/10.1016/j.funeco.2015.06.006.
36. Lima-Mendez G, Faust K, Henry N, Decelle J, Colin S, Carcillo F, et al. Determinants of community structure in the global plankton interactome. Science. 2015;348:1262073.
37. Wemheuer, F., Taylor, J.A., Daniel, R. et al. Tax4Fun2: prediction of habitat-specific functional profiles and functional redundancy based on 16S rRNA gene sequences. Environmental Microbiome 15, 11 (2020). https://doi.org/10.1186/s40793-020-00358-7
38. Houyun Huang, Lei Zhou, Jian Chen and Taiyun Wei (2020). ggcor: Extended tools for correlation analysis and visualization. R package version 0.9.7.
39. Deng, Y., Jiang, Y., Yang, Y. et al. Molecular ecological network analyses. BMC Bioinformatics 13, 113 (2012). https://doi.org/10.1186/1471-2105-13-113
40. Bastian M., Heymann S., Jacomy M. (2009). Gephi: an open source software for exploring and manipulating networks. International AAAI Conference on Weblogs and Social Media.
41. Hillebrand H, Bennett DM, Cadotte MW (2008) Consequences of dominance: a review of evenness effects on local and regional ecosystem processes. Ecology 89:1510–1520
42. Yang LH, Bastow JL, Spence KO, Wright AN (2008) What can we learn from resource pulses. Ecology 89:621–634

43. Daniel A. Vallero (2008) Fundamentals of Air Pollution (Fourth Edition). Pages 786-824
44. María J.DelgadoSergioCasellaEulogio J.Bedmar (2007) Biology of the Nitrogen Cycle. Pages 83-91.

Figures

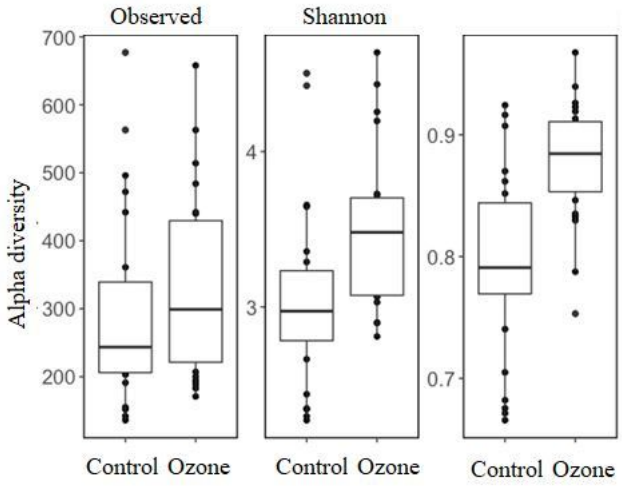

Figure 1

Observed, Shannon, and Simpson diversity indices of samples of the two biofilters.

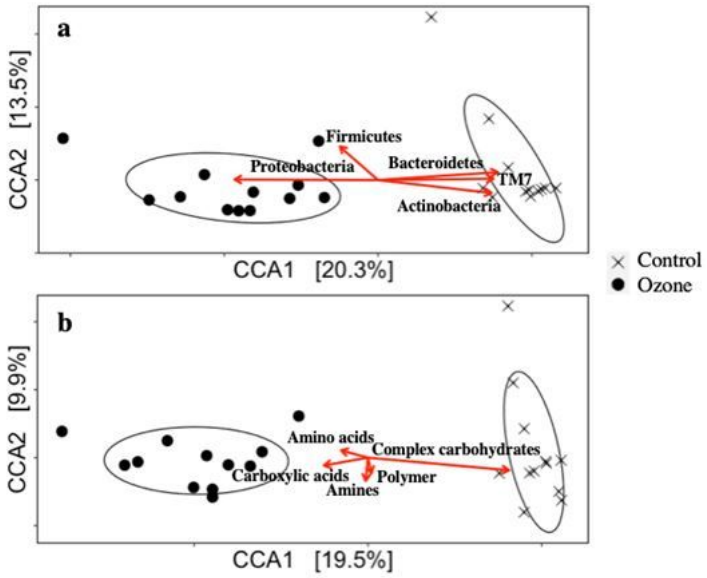

Figure 2

(a) CCA analysis of ASV composition with relative abundance of Actinobacteria, Proteobacteria, Firmicutes, Bacteroidetes, and TM7 as constraining variables. (b) CCA analysis of ASV composition with the metabolic rate of amino acids, carboxylic acids, amines, polymers, and complex carbohydrates as constraining variables

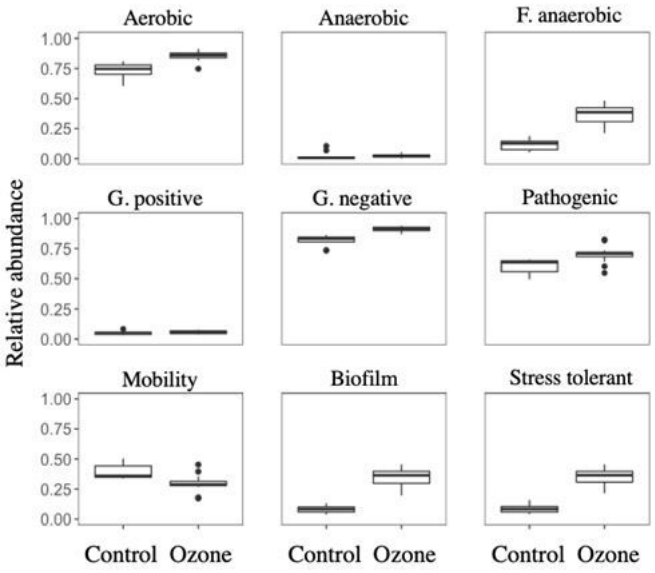

Figure 3

Community functional mapping using the Bugbase database, for quantifying relative abundance of traits in nine categories

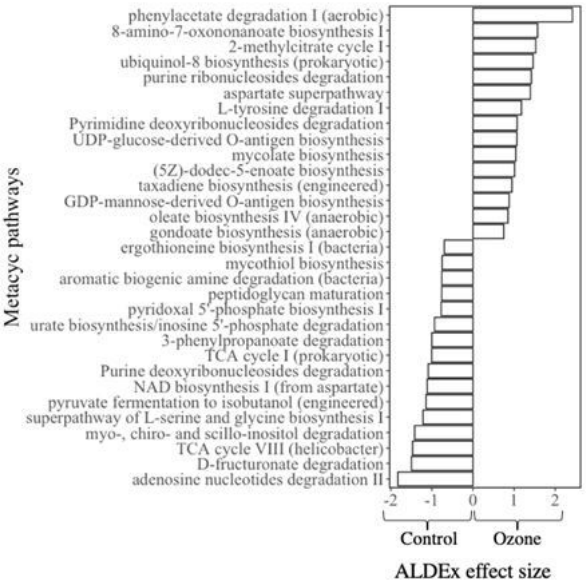

Figure 4

Statistically differentiated MetaCyc pathways predicted by PICRUSt2 and filtered with ALDEx2 corrected Wilcoxon test.

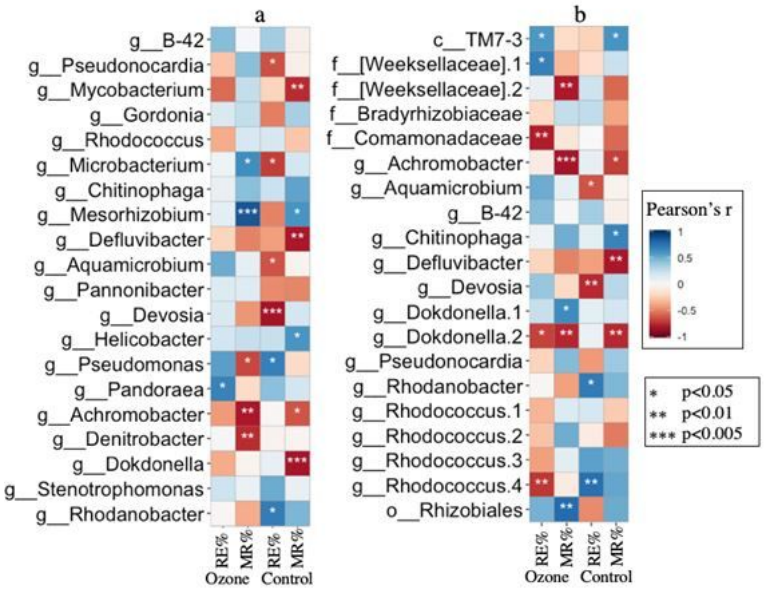

Figure 5

Top 20 taxa in average relative abundance in all samples, and their Pearson correlation with removal efficiency (RE%) and mineralization rate (MR%) in two biofilters. (a) genus level. (b) ASV level, named for the lowest taxa rank identified with confidence over 97%, numbers are appended after names if different ASVs share the same lowest rank name.

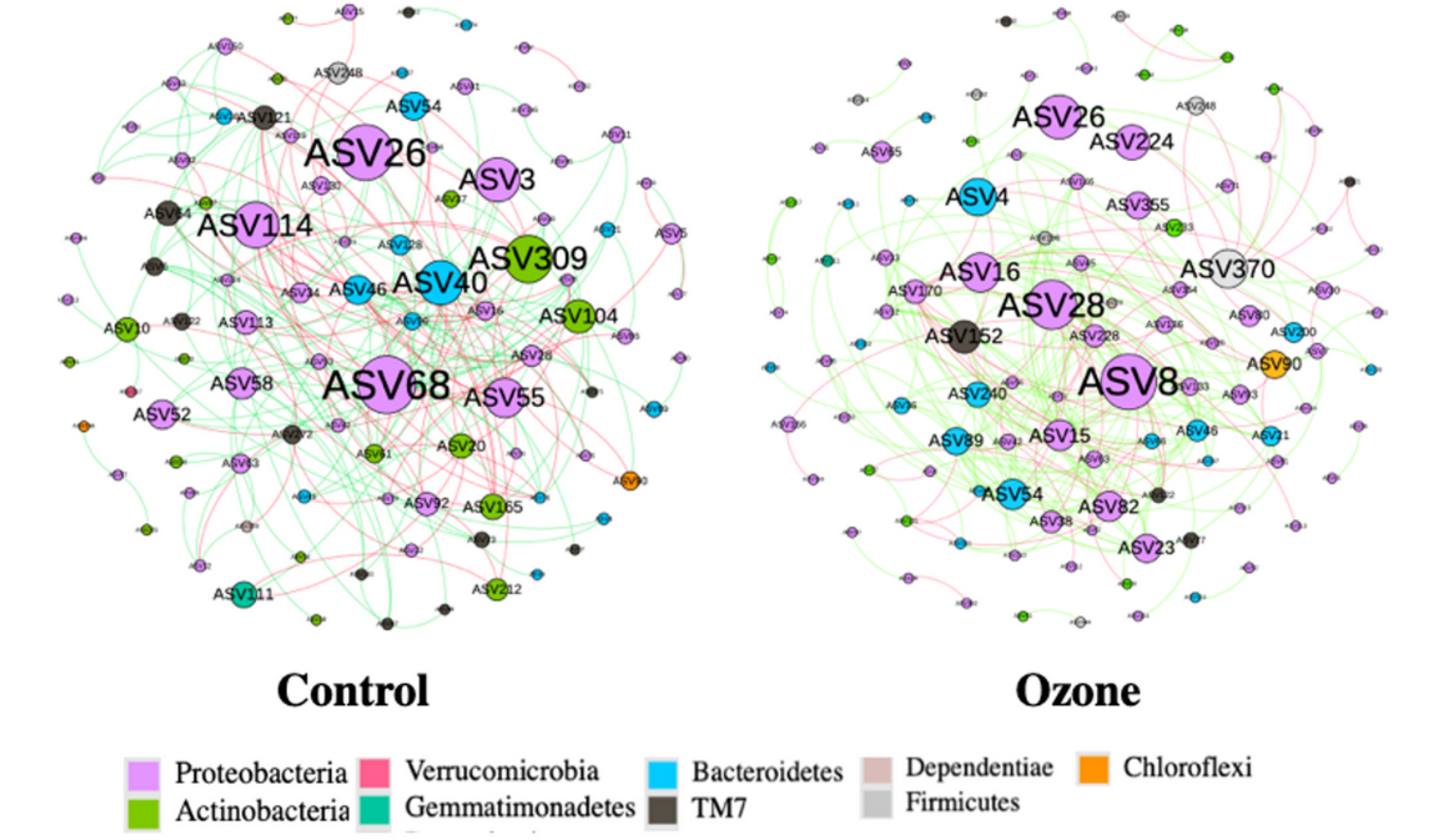

Figure 6

Microbial network in two biofilters with node color as phylum, node size for betweennes and edge color as positive or negative correlations.

Supplementary Files

This is a list of supplementary files associated with this preprint. Click to download.

- sup5lefse.xls
- sup3biolog.xlsx
- sup1betapoints.docx
- sup4taxonomy.tsv
- sup2structure.docx